Ab initio study of Ag/Al_2O_3 and Au/Al_2O_3 interfaces

Jiwei Feng, Wenqing Zhang, and Wan Jiang
State Key Laboratory of High Performance Ceramics and Superfine Microstructure, Institute of Ceramics, Chinese Academy of Sciences, Shanghai, 200050, China

(Received 18 April 2005; revised manuscript received 5 July 2005; published 21 September 2005)

Structural stability, adhesion, and chemical bonding of the Ag(111)/α-Al_2O_3 (0001) and Au(111)/α-Al_2O_3 (0001) interfaces are investigated by an *ab initio* approach based on density functional theory. The interfaces are shown to have different stable structures of Al_2, Al, or O termination depending on the chemical potential of aluminum or oxygen atom. A link to thermodynamic factors, i.e., the partial pressure of oxygen gas or the activity of aluminum, is established based on the *ab initio* thermodynamics developed recently. For condition applicable to sessile drop experiments, the O-terminated interface could exist for the Ag/Al_2O_3 system but be hard to observe for the Au/Al_2O_3 interfaces, consistent with the known experiments. The Al_2 termination is possible for the Au/Al_2O_3 interface at relatively low O_2 pressure or high Al activity but may be hard to form for the Ag/Al_2O_3 interface. Works of adhesion W_{ad} of the stoichiometric interfaces are calculated to be 0.33 J/m^2 in generalized gradient approximation (GGA) and 0.59 J/m^2 in local density approximation (LDA) for the Ag/Al_2O_3 interface, 0.29 J/m^2 in GGA and 0.58 J/m^2 in LDA for the Au/Al_2O_3 interface, in reasonable agreement with measured data.

DOI: 10.1103/PhysRevB.72.115423 PACS number(s): 68.35.Ct, 68.35.Np

I. INTRODUCTION

Metal-alumina interfaces play an important role in many materials that have industrial applications, such as thermal barrier coating for high-temperature gas-turbine engines,[1] heterogeneous catalysis,[2,3] and microelectronics.[4] Structure and adhesion of the interfaces are the two key factors to determine the performance of materials and have stimulated much experimental and theoretical research. Experimentally, sessile drop experiments gave the adhesive energies of the interfaces by measuring the contact angles between metal drops and alumina substrate.[5] Low-energy electron diffraction, scanning tunneling microscopy, and transmission electron microscopy techniques have been applying to extract the structural information of interfaces at nearly atomic resolution.[6–9] High-resolution spectroscopic methods such as high-resolution electron-energy-loss spectroscopy, and x-ray photoemission spectroscopy make it possible to get both the structural information of a metal layer on corundum surface[10,11] and insight into the details of chemical interaction at the interfaces.[12] Theoretically, the metal/Al_2O_3 interfaces are also being studied by different methods (see Finnis's review paper)[13] including thermodynamic modeling based on empirical correlations, image charge model, semiempirical tight-binding method, and Hartree-Fock theory. The most widely used methods are the *ab initio* calculations based on the density functional theory.[13] However, the nature of the adhesion of the metal/oxide interfaces is still not well established.

As is well known, *ab initio* methods describe the energetics of a specific system at an ideal condition of zero temperature very well. However, the effect from temperature, pressure, and other thermodynamic factors on interfacial structure and adhesion has to be considered when an interface is placed in a realistic environment. In recent years, the so-called *ab initio* thermodynamics,[14–17] i.e., the method by combining *ab initio* calculations with thermodynamics, has become an important strategy in structure stability analysis of complex materials.[18–26] These computations cover a wide range of problems in surface structures,[18] defect stability,[19,20] doping[21] of semiconductors, oxide surfaces,[22–25] and metal/oxide interfaces.[15,16,25,26]

By using the *ab initio* thermodynamics, *ab initio* studies were performed for the Nb/Al_2O_3,[25–27] Al/Al_2O_3,[15] Ni/Al_2O_3,[16] and Cu/Al_2O_3 (Ref. 16) interfaces. It was predicted that those metal/Al_2O_3 interfaces may have different termination depending on the oxygen partial pressure or the aluminum activity. Therefore, the interfacial energy, works of adhesion, and works of separation of an interface depend on the condition in which the interface is made, which was shown to agree with experimental measurement.[16,28] Experimental work had already been performed for interfaces formed between Al_2O_3 and different metals, and a qualitative trend between the interfacial works of adhesion and the formation energies of metal oxides was discussed.[29,30] Theoretically, only the interfaces between Al_2O_3 and a few metals including bcc metal Nb and fcc metals Al, Cu, and Ni were studied until now. Note that both Ag and Au have the considerable lower oxide formation energies than that of other metal elements (Cu, Ni, Al).[31] Therefore, the observed and calculated dependence of stabilities and adhesion on environment factors for the $(Ni,Cu)/Al_2O_3$ interfaces[16] may not be applicable to the interface between Al_2O_3 and Ag or Au. From this point of view, it is interesting to work on the $(Ag,Au)/Al_2O_3$ interfaces. To our knowledge, with the exception of Ref. 15, most of the published works on Ag/α-Al_2O_3(0001) interface were based on the model of a single Ag atom or a small Ag cluster instead of a thick metal layer on alumina surface, mainly performed by Zhukovskii *et al.*[32–34] They inferred that the Al-terminated interface has weaker adhesion, and that the O-terminated one has much stronger adhesion due to the ionic bonding at the interface. But, it is not clear that in what conditions the interface is O

terminated or Al terminated. As for the Au/α-Al_2O_3 system, Hernández and Sanz studied the interaction between a single gold atom and the Al-terminated α-Al_2O_3 (0001) surface recently.[35] No *ab initio* work on Au/Al_2O_3 interface was reported until now.

The paper is organized as follows. Section II describes methodology and computational details. Basics of the *ab initio* thermodynamics is also briefly introduced in this section. Section III discusses the structural stability and chemical bonding of the Ag/Al_2O_3 and Au/Al_2O_3 interfaces. Dependence of interfacial stability on oxygen partial pressure and relationship to measurement are presented in Sec. IV.

II. METHODOLOGY

A. Computational details

The electronic calculations are performed using the Vienna *ab initio* simulation program (VASP),[36,37] together with the optimized ultrasoft pseudopotentials.[38,39] Most of the calculations are based on the generalized gradient approximation (GGA)[40] for the exchange correlation (XC) potentials. But, calculations using the local density approximation[41,42] (LDA) for some specific systems are also performed. Comparison of the results in GGA and LDA is made. Extensive tests by us and former researchers have shown the effectiveness of the VASP package,[16,43] a popular plane-wave electronic structure calculation program. To ensure the convergence of results, all calculations are preformed using the same unit cell dimensions, energy cutoff as high as 400 eV for the plane wave basis set, and a $3\times3\times1$ Monkhorst-Pack uniform k-point sampling for integrals over the Brillouin zone.

Test calculations for the bulk and surface properties of Ag, Au, and Al_2O_3 are performed at first to assess the accuracy of the pseudopotentials used for interface systems. The equilibrium lattice constants are obtained to be 4.17 Å (GGA) and 4.04 Å (LDA) for Ag, 4.18 Å (GGA) and 4.08 Å (LDA) for Au, and 4.77 Å in both LDA and GGA for Al_2O_3 bulk. They all agree very well with previous *ab initio* calculations and measured data.[43–47] Surface energy calculations are performed using both (1×1) and $(\sqrt{3}\times\sqrt{3})R30°$ surface unit cells for Ag (111) and Au (111) surfaces. Only the (1×1) cell is used for Al_2O_3 (0001) surface. The obtained surface energies of Ag or Au in the different unit cell approach agree with each other very well. They are 0.798 J/m^2 in GGA and 1.211 J/m^2 in LDA for Ag, 0.808 J/m^2 in GGA and 1.218 J/m^2 in LDA for Au, and 1.68 J/m^2 in GGA and 2.00 J/m^2 in LDA for the Al-terminated Al_2O_3(0001) surface. They are also consistent with previous calculations.[43–47] Notice that the surface energy of a system in GGA is normally 20–30 % lower than the corresponding one in LDA, which was also found and discussed before.[43,48] The reason is that GGA may have a problem when dealing with edge electronic gas close to surface.[49] For the Al_2O_3 (0001) surface, the calculated interlayer relaxations also show consistency with earlier DFT studies[24,43,48] but are not presented here for brevity. Again, the Al-terminated Al_2O_3 (0001) surface is proved to be the most stable one among all the possible surfaces within the physically acceptable range of chemical potential of oxygen.[24,25]

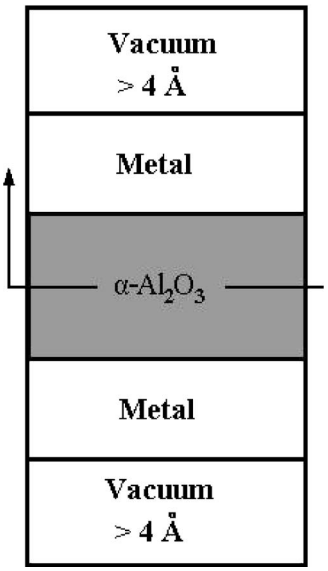

FIG. 1. Schema of the sandwiched interface supercell used in calculations. The central part of the interface is α-Al_2O_3. Ball models of the upper parts of the interfaces with different terminations are shown in Figs. 3(a)–3(c).

Supercell approach is employed to simulate the $(Au,Ag)/Al_2O_3$ interfaces. The interfacial supercell, as shown in Fig. 1, has a sandwich configuration with an alumina layer between two metal slabs, separated by a vacuum of thickness more than 8 Å. The supercell contains two equivalent interfaces of the same O, Al, or Al_2 termination. Each metal slab has four atomic layers, and the central alumina has six O layers and twelve Al layers for the Al-terminated interface. Adding or removing an aluminum layer onto the Al-terminated Al_2O_3 surface leads to the Al_2-terminated or the O-terminated interface model. The Al-terminated, Al_2-terminated, and O-terminated interfaces are labeled as $(Ag,Au)/(Al_2O_3)_{Al}$, $(Ag,Au)/(Al_2O_3)_{Al2}$, and $(Ag,Au)/(Al_2O_3)_O$, respectively. The interfacial orientation is metal(111)/α-Al_2O_3(0001) for both Ag and Au systems, the same as the $(Al,Ni,Cu)/Al_2O_3$ interfaces as observed experimentally and used before.[43,50,51]

Because of the relatively large lattice mismatch between either Ag(111) or Au(111) and Al_2O_3(0001), the effect of misfit strain must be estimated. A unit cell that includes misfit dislocations[52] is obviously beyond the present computational capabilities for these systems. Our approach is as follows. We consider four commensurate interfaces with different imposed strains, two for GGA calculations (GGA type-I and GGA type-II) and another two for LDA calculations (LDA type-I and LDA type-II). In each, the lattices of the metal or oxide (or both) are expanded/compressed in plane, (111)/(0001), and the entire slab relaxed freely. By using these configurations, we attempt to span the local interatomic structures found in experimental interfaces. This misfit generates a strain energy that depends on the volume of the strained lattice. It represents an extremely important contribution to the overall energy of the system containing

TABLE I. Strains in the metal and Al_2O_3 at the type I and type II interfaces: "+" designates stretched, and "–" compressed. The lattice constant is for the two-dimensional cell of the matched interface. The reference lattice constant for Al_2O_3 is taken to be the experimental value 4.7628 Å and that for Ag and Au are calculated in either GGA or LDA. They are 4.17 Å (GGA) and 4.04 Å (LDA) for Ag and 4.18 Å (GGA) and 4.08 Å (LDA) for Au.

Interface types		In-plane lattice constant of supercell (Å)	Strain (%) Ag	Au	Al_2O_3
GGA	type I	4.7628	−6.70	−7.00	0.00
	type II	4.9285	−3.50	−3.80	+3.50
LDA	type I	4.7628	−3.72	−4.69	0.00
	type II	4.9285	−0.37	−1.37	+3.50

the interface. To disassociate this contribution from the interface energy, the present calculations compare the ensemble energy with that for the bulk materials, subject to the same imposed strain, at the same volume. The difference between the ensemble and the two bulk materials then isolates the interface energy from other contributions to the total energy. Ultimately, only the results that are not sensitive to the interface strain are trusted. The approach was proposed by Zhang *et al.* and has been applied in the study of $(Ni,Cu)/Al_2O_3$ interfaces with and without impurities.[16]

The four types of commensurate interfaces are as follows. In GGA, type-I interface corresponds to fixing the Al_2O_3 at its experimental lattice constant 4.7628 Å,[53] but to compressing metal lattice, 6.7% for Ag and 7% for Au. Type-II interface model is built by stretching Al_2O_3 by 3.5% and compressing Ag by 3.5% (Au by 3.8%). In LDA, type-I interface corresponds to compressing 3.73% for Ag and 4.69% for Au but to fixing Al_2O_3 at its experimental lattice constant. LDA type-II interface model is formed by expanding Al_2O_3 by 3.5% and compressing Ag by 0.37% and Au by 1.37%. Note that the compression of metal slabs to form commensurate interfaces in LDA is much smaller than that in GGA. This is due to the fact that GGA often overestimates lattice constants of solids. LDA interfaces have mismatch around 4%. Compression of metal lattice is much less than that in GGA to form commensurate interfaces (see Table I).

To avoid metastable states of the complex interfaces, Ag or Au slab is slid on the Al_2O_3 surface to get different initial interfacial structures. At least three kinds of initial configurations are employed for our calculations. They correspond to the Ag or Au atoms on top of Al atoms (labeled as the Al top), on top of oxygen atoms (O top), or on top of the threefold oxygen hollow sites (hollow-top), respectively (see Fig. 2). All the structures are fully relaxed by minimizing the Hellmann-Feynman forces on all the atoms to less than 0.01 eV/Å.

B. Link to thermodynamic quantities

Similar to the $(Cu,Ni)/Al_2O_3$ interfaces studied before,[16] the stability of the complex $(Ag,Au)/Al_2O_3$ interfaces depends on the chemical potential of Al μ_{Al} or the chemical potential of oxygen μ_O. We only describe the link of *ab initio* results to thermodynamic quantities briefly here, and readers may refer to our earlier publications[16,17] for details. When thermodynamic equilibrium exists at the metal $(M)/Al_2O_3$ interface, the interfacial Gibbs energy G_I at temperature T, is related to the free energy of the ensemble (at ambient pressure) by[16]

$$G_I = G_{\text{total}} - \tfrac{1}{3}N_O\mu^0_{Al_2O_3} - N_M\mu_M - \left[N_{Al} - \frac{2}{3}N_O\right]\Delta\mu_{Al} - \left[N_{Al} - \frac{2}{3}N_O\right]\mu^0_{Al}(0\ \text{K}), \quad (1)$$

where G_{total} is the total energy of the interface ensemble. μ_O, μ_{Al}, and μ_M are the chemical potentials of O, Al, and metal atoms, respectively, and N_O, N_{Al}, N_M are the corresponding numbers of atoms. $\Delta\mu_{Al}$ is defined by $\Delta\mu_{Al}$

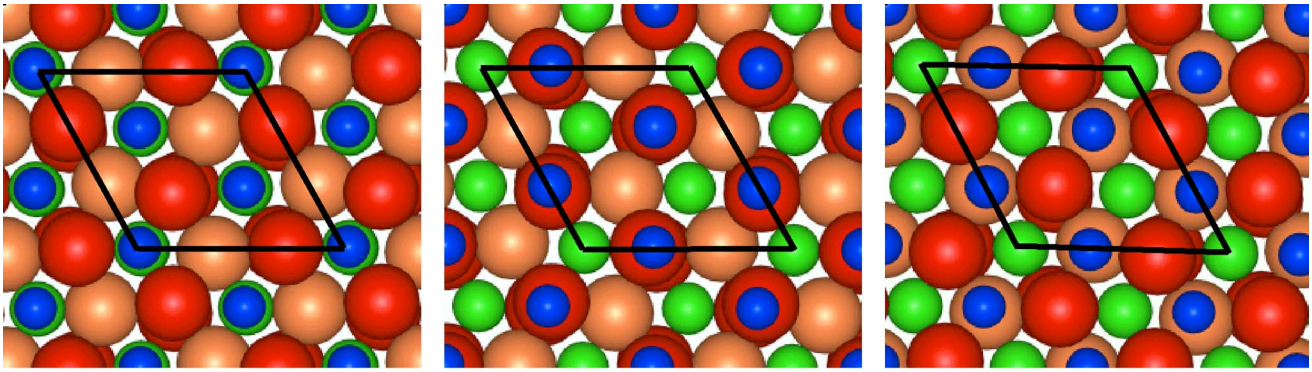

FIG. 2. (Color online). Ball models of three interfacial configurations before relaxation (top view). Small black (blue in color) balls represent metal (Ag or Au) atoms; small gray (green in color) balls represent Al atoms; big black (red in color) balls represent the first-layer O atoms close to the interface plane; big gray (orange in color) balls represent the second layer O atoms. Dark lined parallelograms show the surface unit cell used in calculations. (a) Metal atoms on top of Al atoms (Al top); (b) Metal atoms on top of O atoms (O top); (c) Metal atoms on top of the threefold oxygen hollow sites (hollow top).

$=\mu_{Al}-\mu^0_{Al}(0\ K)$, where $\mu^0_{Al}(0\ K)$ is the chemical potential of the *ab initio* standard state of fcc Al at zero temperature.[16] The superscript 0 refers to the quantities for pure bulk solids. To get Eq. (1), the Al and O at the interface (both in solid solution in the metal and at the termination of the Al_2O_3) are assumed to be in equilibrium with bulk Al_2O_3 and with the metal. The metal (M) atoms at the interface are also assumed to be at equilibrium with a metal bulk. Therefore, the conditions of $\mu_M=\mu^0_M(T)$ and $3\mu_0+2\mu_{Al}=\mu^0_{Al_2O_3}(T)$ can be adopted in deriving Eq. (1). Interfacial energies and their dependence on the aluminum chemical potentials can be calculated by using Eq. (1) and taking *ab initio* total energies as input. The structure with the lowest interfacial energy is the most stable one. Relationship of G_I to aluminum activity a_{Al} and to oxygen partial pressure P_{O2} at finite temperature can be established by[16,17]

$$\Delta\mu_{Al}=kT\ln a_{Al}+\Delta^0_{Al}(T), \tag{2}$$

$$\frac{3}{2}\ln P_{O_2}=\frac{1}{kT}\Delta G^0_{Al_2O_3}(T)-2\ln a_{Al}, \tag{3}$$

where k is Boltzmann constant, $\Delta^0_{Al}(T)$ is defined by $\Delta^0_{Al}(T)=\mu^0_{Al}(T)-\mu^0_{Al}(0\ K)$ and is calculated based on the JANAF table.[17,54] $\Delta G^0_{Al_2O_3}$ is the experimental standard Gibbs reaction energy for α-Al_2O_3 formation in accordance with the reaction $2Al(solid)+3/2\ O_2(gas)=Al_2O_3(solid)$, which has been measured and tabulated in a handbook.[55] The temperature dependent chemical potentials of pure solids $\mu^0_X(T)=\mu^0_X(0\ K)+\Delta^0_X(T)$ (X=Au, Ag, Al_2O_3), are employed to calculate the interfacial energy at a finite temperature. $\mu^0_X(0\ K)$ is obtained by *ab initio* method for the stable phase of a solid at 0 K, and the $\Delta^0_X(T)$ term is evaluated by using JANAF table.[54] Note that the aluminum activity is taken as a bridge to link *ab initio* results to the thermodynamic quantities [see Eqs. (2) and (3)]. This is one of the advanced methods developed recently for *ab initio* thermodynamics because it avoids the problem of defining the *ab initio* standard state of oxygen gas.[17]

III. INTERFACIAL STRUCTURE AND CHEMICAL BONDING

A. Interfacial structure

(1) *The Ag/Al_2O_3 interfaces*. As mentioned in Sec. II, we start the relaxation of interfacial structures from three different initial configurations for each of the Al-terminated, O-terminated, and Al_2-terminated interfaces and label them as Al, O, and hollow top, respectively. The most stable configurations for all the type-I and type-II interfaces are presented in Table II. For the O-terminated interface, the Al-top configuration always has the lowest interfacial energy for both the type-I and type-II interfaces. The Ag layer close to the top oxygen layer of Al_2O_3 surface buckles [Fig. 3(b)], and one of the Ag atoms (Ag1 labeled in Fig. 3(b)] occupies the top Al site on the Al_2O_3 surface. The whole first-layer Ag atoms assume the epitaxial positions of the Al sublattice in Al_2O_3 bulk. This was also found for $(Al,Cu)/Al_2O_3$ interfaces before.[16,34,43] The reason is that the Ag1 atom at the Al site saturates the surface oxygen dangling bonds well and

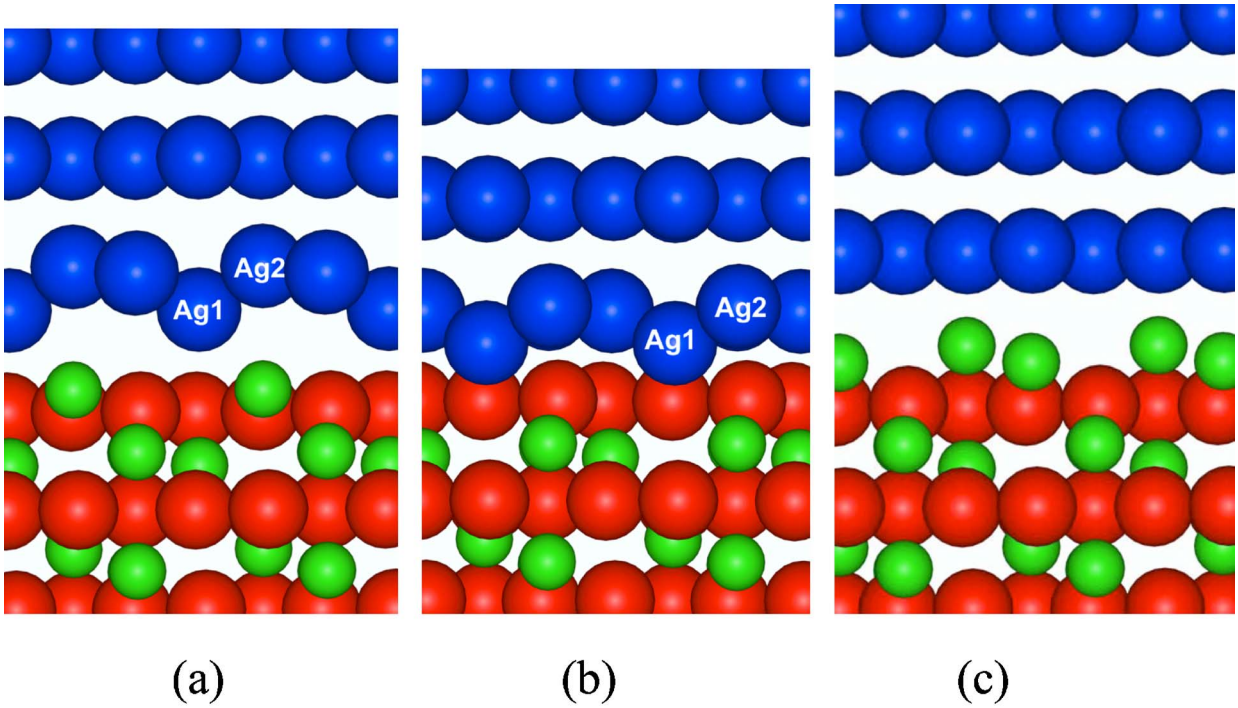

FIG. 3. (Color online). Ball model of the relaxed type-I Ag/Al_2O_3 interfaces (upper half of the symmetric slabs). Big black (blue in color) balls represent Ag atoms, smaller gray (green in color) balls represent Al atoms, and less dark (red in color) balls represent O atoms. Only the most stable configurations are presented. (a) Al-terminated interface of Al top; (b) O-terminated interface of Al-top; (c) Al_2-terminated interface of hollow top.

TABLE II. The most stable configurations for the Ag/Al_2O_3 and Au/Al_2O_3 interfaces. Only GGA results are shown here.

		Al terminated	O terminated	Al_2 terminated
Ag/Al_2O_3	type I	Al top	Al top	hollow top
	type II	O top	Al top	hollow top
Au/Al_2O_3	type I	Al top	Al top	hollow top
	type II	O top	O top	hollow top

therefore stabilizes the O-terminated interface. For the Al-terminated interface [Fig. 3(a)], the Al-top configuration is the most stable one for the type-I interface, and the first-layer Ag atoms also occupy the epitaxial positions of the Al sublattice. It is noticed that the stable interfacial configuration changes to O-top for the Al-terminated type-II interface, but interfacial energy difference from that of the Al top is very small. For the Al_2-terminated interfaces [Fig. 3(c)], both type-I and type-II interfaces stabilize at the hollow-top.

(2) *The Au/Al_2O_3 interface*. In general, the Au/Al_2O_3 interfaces show the same behavior as the Ag/Al_2O_3 interfaces. For the Al-terminated interface, the Au atoms close to the Al_2O_3 locate at the top Al sites for the type-I interface. For the Al_2-terminated interfaces, results are the same as those for the Ag/Al_2O_3 interfaces (see Table II). For the O-terminated interface, the most stable configuration is still the Al-top for type I but change to O-top for type-II interfaces. Similar to the Ag/Al_2O_3 system, the interfacial energy difference between the Al-top and O-top interfaces is marginal. Therefore, type-I interfaces are chosen as the example to discuss the characteristics of chemical bonding at the $(Ag, Au)/Al_2O_3$ interfaces in the following.

B. Chemical bonding at interface

Electron charge density difference contour plots of $(11\bar{2}0)$ plane of the Ag/Al_2O_3 interfaces are presented in Fig. 4. The $(11\bar{2}0)$ plane is chosen because it passes through the interfacial Al and Ag atoms. The relatively black region with solid lines implies electron accumulation in this area, and the relatively white color with dotted lines indicates electron depletion. For the Al-terminated interface [Fig. 4(a)], the interface shows somewhat metallic bonding in addition to the ionic bonding characteristics from the pattern of charge depletion and accumulation around interfacial atoms, especially the Al and oxygen atoms. Figure 5(a) shows the projected density of states (PDOS) of some interfacial atoms. By comparing the PDOS of the interfacial Ag atoms (Ag1 and Ag2) to that of an Ag atom in its bulk state, the *d*-orbital DOS narrows and shifts a little closer to the Fermi level. Integral of the DOS of the Ag in bulk, Ag1 and Ag2 atoms at interface gives nearly the same electron number of the fully occupied *d* orbitals. The Ag *d* electrons do contribute to the interfacial bonding but most possibly redistribute themselves in different orbital. This picture is consistent with the charge density redistribution as shown in Fig. 4(a). Such charge redistribution leads to the polarization force[15,16] as discussed before.

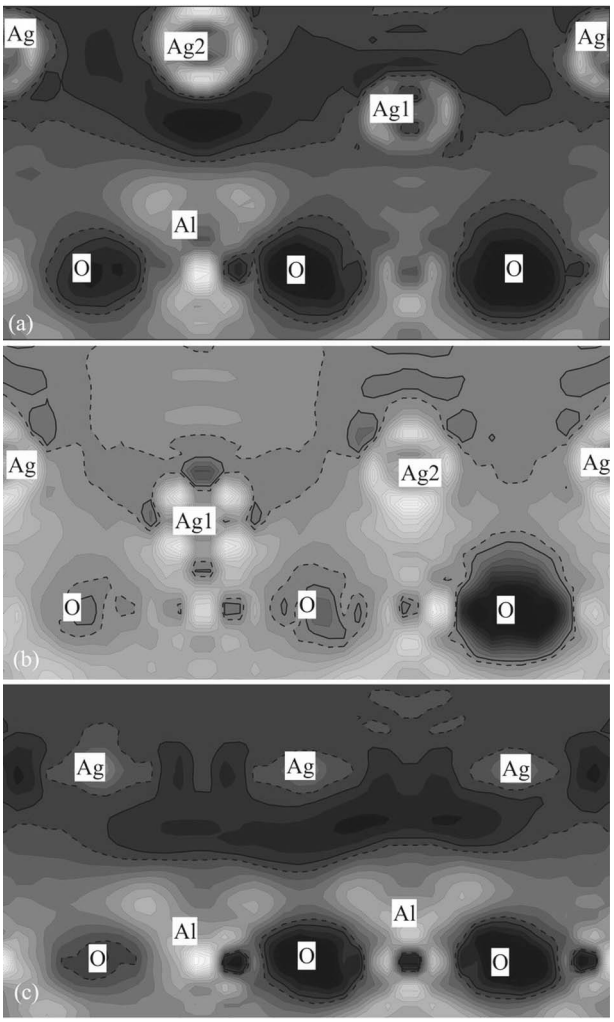

FIG. 4. Electron-density difference contour plots of $(11\bar{2}0)$ plane through interfacial Al and Ag atoms for (a) Al-terminated Ag/Al_2O_3 interface, (b) O-terminated Ag/Al_2O_3 interface, and (c) Al_2-terminated Ag/Al_2O_3 interface. This plot represents the difference between the self-consistent electron density distribution of the solid interface and the sum of the overlapping atomic density distributions. The relatively black area with solid lines indicates electron accumulation, and the relatively white area with dashed lines indicates charge depletion.

Therefore, the chemical bonding at the Al-terminated interface is a combination of both metallic interaction and electron polarization. For the O-terminated interface, the primary bonding is the ionic interaction between Ag and O ions as clearly seen in Fig. 4(b). The PDOS in Fig. 5(b) also shows the overlapping of the *p* electronic states of interfacial O atoms with the *d* electronic states of the Ag1 [Fig. 4(b)] atoms at Fermi energy, indicating covalent interaction between the interfacial Ag and O atoms. For the Al_2-terminated interface, interfacial interaction between the Ag atoms and Al ions are mostly metallic bonds as seen in both Figs. 4(c) and 5(c).

The chemical bonding at the Au/Al_2O_3 interfaces is also analyzed by charge density difference contour plots and project DOS plots. In general, the bonding characteris-

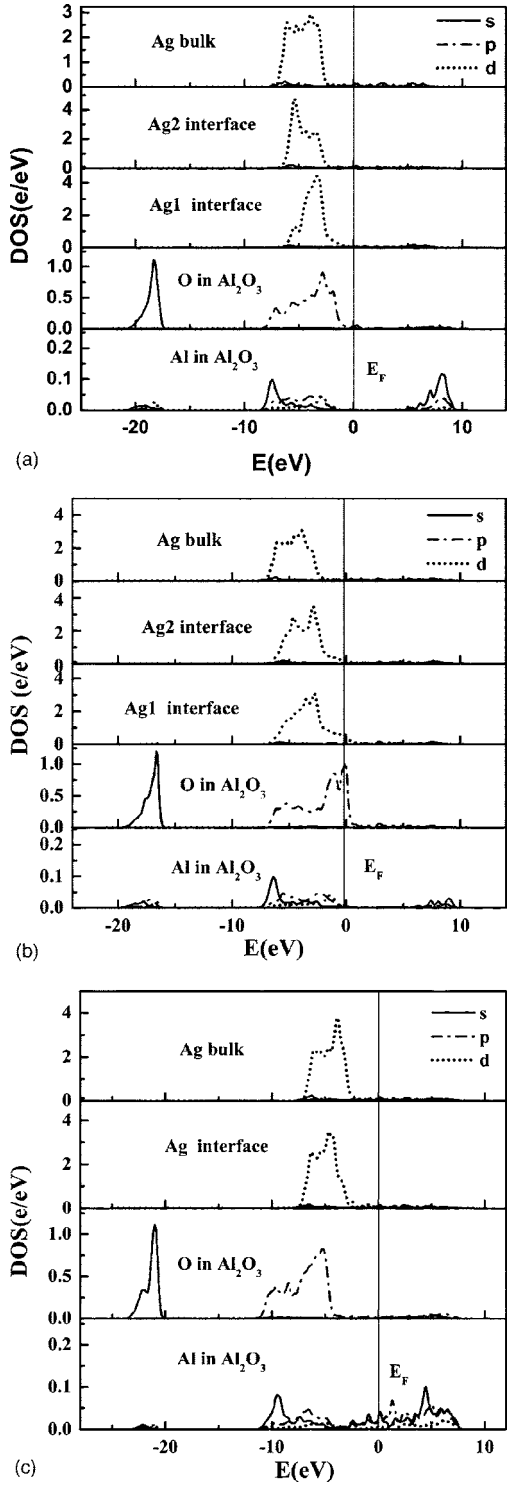

FIG. 5. (a) Projected density of states of interfacial atoms at the Al-terminated Ag/Al_2O_3 interface. Ag1 and Ag2 correspond to the atoms as labeled in Fig. 3(a). Oxygen and Al atoms at the interface have similar DOS distribution to the corresponding atoms in Al_2O_3 bulk. (b) Projected density of states of interfacial atoms at the O-terminated Ag/Al_2O_3 interface. Ag1 and Ag2 correspond to the atoms in Fig. 3(b). (c) Projected density of states of interfacial atoms at the Al_2-terminated Ag/Al_2O_3 interface. The DOS of the three Ag atoms at the interface is similar to the DOS of a Ag atom in its bulk state.

tics of the Al-terminated, O-terminated, and Al_2-terminated Au/Al_2O_3 interfaces are quite similar to that of the Ag/Al_2O_3 interfaces and are not discussed here.

IV. INTERFACIAL STABILITY AND RELATIONSHIP TO MEASUREMENT

A. Interfacial stability

The relationship between the interfacial energy γ_I and the chemical potential of aluminum $\Delta\mu_{Al}$ is plotted in Fig. 6. Note that the $\Delta\mu_{Al}$ is defined by referring to the *ab initio* standard state of fcc Al at zero temperature.[16,17] Only the results for the most stable configurations are presented for each interfacial stoichiometry. The top label $(\ln P_{O_2})$ is a thermodynamic variable, and its link to $\Delta\mu_{Al}$ at a finite temperature is determined by Eqs. (2) and (3). As is known, the condition in which alumina can exist is

$$\Delta\mu_{Al} \leqslant 0 \text{ and } \Delta\mu_O \leqslant 0.$$

The two conditions lead to the physically effective range of $\Delta\mu_{Al}$,

$$-\tfrac{1}{2}\Delta H_{Al_2O_3} \leqslant \Delta\mu_{Al} \leqslant 0, \tag{4}$$

where $\Delta H_{Al_2O_3}$ is the heat of formation of alumina, which is taken to be 17.37 eV.[25] These two limits are presented by the left Y axis and the right vertical dotted line in the figure. It is clear that both type-I and type-II interfaces in both LDA and GGA show the same trend of dependence of the interfacial energy γ_I on $\Delta\mu_{Al}$ for either Ag/Al_2O_3 or Au/Al_2O_3 interface. It means that the strain involved in the ideally commensurate interface model does not affect the trend of interfacial stability for the systems studied here. It should be addressed that the range of $\Delta\mu_{Al}$ for the type-II interfaces with strained Al_2O_3 is a little different from that for type-I interfaces because of the change of $\Delta H_{Al_2O_3}$ with the internal strain in Al_2O_3. Fortunately, our calculations show that the $\Delta H_{Al_2O_3}$ changes very little for the strained Al_2O_3 investigated here. With 3.5% stretching of Al_2O_3 in (0001) plane, $\Delta H_{Al_2O_3}$ of the strained Al2O3 is 17.24 eV/formula in GGA, and 17.04 eV/formula in LDA, only 0.13 eV (GGA) and 0.28 eV (LDA) difference from 17.37 eV for the unstrained Al_2O_3. Therefore, we still use the thermodynamic parameters for the unstrained Al_2O_3 to discuss problems in this paper.

Similar to $(Ni,Cu)/Al_2O_3$ interfaces,[16] as $\Delta\mu_{Al}$ decreases, the Al_2-terimated, Al-terminated, or O-terminated interfaces becomes the most stable one, respectively. The O-terminated $Au/(Al_2O_3)_O$ interface needs much lower $\Delta\mu_{Al}$ value to be stable comparing with that for the $Ag/(Al_2O_3)_O$ interfaces. This is consistent with the chemical bonding picture (see Sec. III B). The bonding at the O-terminated interfaces is mainly from the interaction between O atoms and metal atoms. As is known, Ag can form an oxide with $\Delta H_{Ag_2O} = -0.32$ eV (per O atom),[31] but Au has no oxide. The energies for the Al-terminated interfaces are independent of $\Delta\mu_{Al}$. For both the $Ag/(Al_2O_3)_{Al}$ and $Au/(Al_2O_3)_{Al}$ interfaces, the range of $\Delta\mu_{Al}$ in which the Al-terminated interface can exist is relatively wide so that the Al-terminated inter-

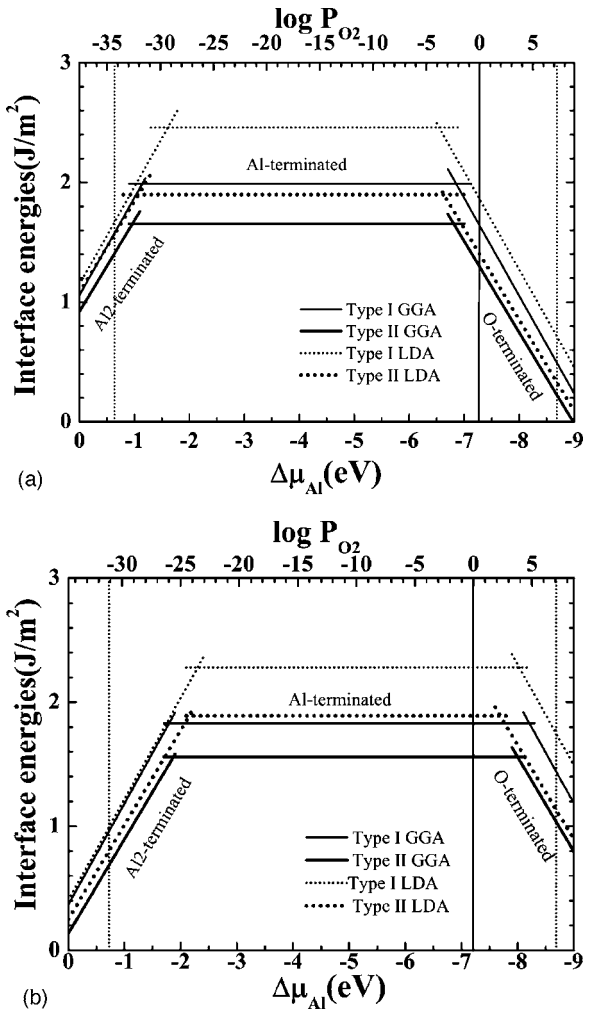

FIG. 6. Interfacial energies γ_I of type-I and type-II interfaces for (a) Ag/Al_2O_3 and (b) Au/Al_2O_3. The oxygen partial pressure are inferred from the $\Delta\mu_{Al}$ by the combination of Eqs. (2) and (3) at a experimental temperature 1300 K for Ag/Al_2O_3 and at 1400 K for Au/Al_2O_3. The left vertical dotted line represents the limit that aluminum activity should be less than 1 at the experimental temperature. The right vertical dotted lines are defined by $\Delta\mu_O < 5.79$ eV.

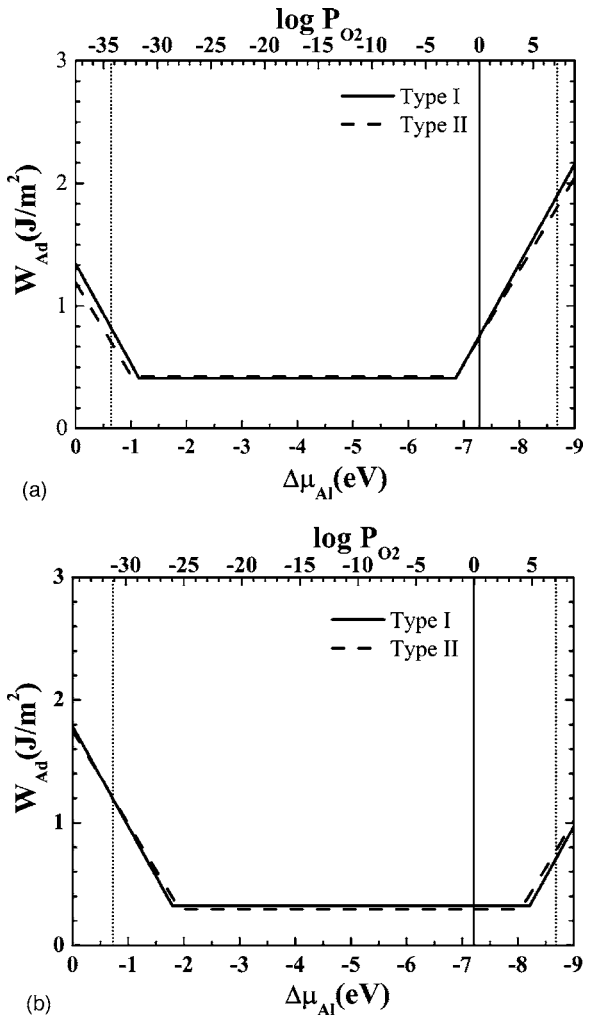

FIG. 7. Works of adhesion for (a) Ag/Al_2O_3 interfaces at 1300 K and (b) Au/Al_2O_3 interfaces at 1400 K. Only the results in GGA are plotted.

faces should be able to be obtained easily in comparison with either the O-terminated or the Al_2-terminated interfaces. The $(Ag,Au)/(Al_2O_3)_{Al2}$ interfaces can exist only if $\Delta\mu_{Al}$ is very high due to basically the weak bonding between Ag(Au) and Al atoms. This is consistent with observation that there is no naturally existed stable Ag-Al and Au-Al alloys. Calculations in LDA for interfacial energies are also performed for the type-I $(Au,Ag)/Al_2O_3$ interfaces, and the last results are presented in Fig. 6 together with the GGA results. It is not a surprise that LDA calculations give the same trend of interfacial stability as that from GGA calculations, similar to what we obtained before for Nb/Al_2O_3 interfaces.[25]

B. Relationship to measurement

Figures 6(a) and 6(b) also show the dependence of the interfacial energy γ_I on the oxygen partial pressure P_{O_2} determined from $\Delta\mu_{Al}$ by the combination of Eqs. (1)–(3). The temperature used is 1300 K for Ag/Al_2O_3 in Fig. 6(a) and 1400 K for Au/Al_2O_3 in Fig. 6(b), at which most sessile drop measurements were performed.[56,57] The left dotted vertical lines in Figs. 6(a) and 6(b) correspond to $a_{Al}=1$. The corresponding works of adhesion W_{Ad} of the $(Ag,Au)/Al_2O_3$ interfaces and their dependence on oxygen partial pressure P_{O_2} are obtained from the interfacial energies in conjunction with the surface energies ($\sigma_{(Al_2O_3)_{Al}}$ and σ_M) upon using:

$$W_{Ad} = \sigma_M + \sigma_{(Al_2O_3)_{Al}} - \gamma_I, \tag{5}$$

where $\sigma_{(Al_2O_3)_{Al}}$ is the surface energy of the most stable Al_2O_3 surface (Al terminated) and σ_M represents the surface energy of metal surface. Both surfaces have the same strain as they have in the corresponding interfaces. The results of W_{ad} in GGA are presented in Fig. 7(a) for Ag/Al_2O_3 and in Fig. 7(b) for Au/Al_2O_3 interfaces. Interestingly, the type-I and type-II interfaces almost have the identical works of adhesion. The small difference of the slopes of the W_{ad} curves

TABLE III. Works of separation $W_{sep}(J/m^2)$ for the $(Ag,Au)/Al_2O_3$ interfaces. Results for metal (M/M) and $Al_2O_3(Al_2O_3/Al_2O_3)$ are for the bulk at the corresponding strained states. $M/M(Al_2O_3)_O$ represents that one-third of the metal atoms in the layer close to interface plane are left on the O-terminated alumina surface. The data outside of the parentheses are calculated by Eq. (6b) and the data in the parentheses are calculated by Eq. (6a).

	Model type	$M/(Al_2O_3)_{Al}$	Expt. data	$M/(Al_2O_3)_O$		$M/(Al_2O_3)_{Al2}$	M/M	Al_2O_3/Al_2O_3
				$M/(Al_2O_3)_O$	$M/M(Al_2O_3)_O$			
	II (GGA)	0.32 (0.42)	0.50[a]	4.10 (4.20)	2.06	1.85 (1.95)	1.59	2.56
Ag	I (GGA)	0.33 (0.41)		3.93 (4.00)	2.53	1.83 (1.93)	1.44	3.36
	II (LDA)	0.83 (0.91)		5.14 (5.31)		2.55 (2.54)	2.42	3.19
	I (LDA)	0.59 (0.75)		5.00 (5.12)		2.56 (2.68)	2.43	4.00
	II (GGA)	0.21 (0.29)	0.6-0.9[b]	3.08 (3.16)		2.42 (2.51)	1.14	2.56
Au	I (GGA)	0.29 (0.32)	0.3-0.43[c]	2.78 (2.81)	1.46	2.31 (2.38)	0.95	3.36
	II (LDA)	0.73 (0.88)		4.23 (4.47)		3.27 (3.33)	2.34	3.19
	I (LDA)	0.58 (0.65)		3.78 (3.80)		3.12 (3.42)	1.86	4.00

[a]Reference 56.
[b]Reference 58.
[c]Reference 57.

for the O-terminated and the Al_2-terminated interfaces is from the change of the in-plane lattice constants at the different strained interfacial states. This is due to the fact that the strain effect on surface energies and that on interfacial energy are nearly equal. When Eq. (5) is applied to calculate W_{ad}, the strain effects on surfaces and interface cancel each other. The same phenomenon is also observed in the calculations of works of separation (see Table III) for the type-I and type-II interfaces.

1. Al-terminated and O-terminated interfaces

We first make a comparison of the calculated works of separation (W_{sep}) with the measured one. W_{sep} can be calculated in two approaches. One way is to obtain W_{sep} by

$$W_{sep} = \sigma_M + \sigma_{Al_2O_3} - \gamma_I. \tag{6a}$$

This is just the definition of work of separation of an interface that is separated to give two surfaces. Although Eq. (6a) is similar to Eq. (5), the term $\sigma_{Al_2O_3}$ in Eq. (6a) does not correspond to the most stable Al-terminated Al_2O_3 surface as Eq. (5) does. It is the Al_2O_3 part of an interface after the interface is separated. In order to get W_{sep} using Eq. (6a), $\sigma_{Al_2O_3}$ for Al_2O_3 surfaces of different terminations have to be calculated.[25] $\sigma_{Al_2O_3}$ and γ_I have the same dependence on partial pressure of Al or oxygen atom, therefore, Eq. (6a) gives a fixed value of W_{sep}. Another approach is to get W_{sep} by

$$W_{sep} = (E_1 + E_2 - E_{total})/2A, \tag{6b}$$

where E_{total} is the total energy of an interface supercell that contains both metal and Al_2O_3 slabs. $E_1(E_2)$ is the total energy of a supercell that has the same dimensions as the interface supercell but contains only the metal (the Al_2O_3) slab. A is the cross-sectional area of the supercell. Both approaches give close values for W_{sep}, and the results from both Eqs. (6a) and (6b) are presented together in Table III.

Because the Al-terminated interface is stoichiometric, work of separation of the interface W_{sep} is the same as W_{ad} that has been measured in the passed years.[56–58] Notice that the experimental values of W_{sep} fall between the LDA and GGA results of W_{sep}. For the $Ag/(Al_2O_3)_{Al}$ interface, LDA value is closer to the measured one. By taking account of the effect that GGA calculations underestimate surface energy,[49] we believe that the LDA result is more reasonable. In that case, the calculated work of separation show a reasonable agreement with the measured value. For the $Au/(Al_2O_3)_{Al}$ interface, our LDA result is higher than the experimental values from sessile drop experiments[57] but close to the one obtained by dihedral angle measurement.[58] Compare to both the O-terminated and Al_2-terminated interfaces, the Al-terminated interface has a relatively low W_{sep}. This is partially due to the fact that the bonding at the interface is mainly from weak metallic interaction and polarization, which are not as strong as the ionic bonding at the O-terminated interface or the metallic bonding at the Al_2-terminated interfaces.

The Al-terminated Ag/Al_2O_3 interface is estimated to be stable when P_{O_2} is in the range of 10^{-33}–10^{-3} atmosphere [Fig. 6(a)]. The O-terminated interface becomes the most stable one after oxygen partial pressure exceeds $\sim 10^{-2}$ atmosphere. Experimentally, Chatain *et al.* observed that the contact angle of Ag drops on Al_2O_3 surface was a constant at relatively low oxygen partial pressure but kept decreasing after oxygen partial pressure was above a critical value in a careful sessile drop experiment,[56] indicating the transition of the interfacial structure from Al-terminated to O-terminated one. This is consistent with our theoretical prediction. One thing that should be mentioned is that two plateau areas were observed in experiment (as shown in Fig. 4 of Ref. 56) with a small difference of works of adhesion. We do not under-

stand that well but guess that the difference may come from possible reconstruction of the stoichiometric interfaces.

The O-terminated Ag/Al_2O_3 interface can exist after oxygen partial pressure $P_{O_2} > 10^{-3}$ atmosphere based on our theoretical estimation. Sessile drop measurements carried out in the range of oxygen partial pressure did find a decreasing of contact angle, corresponding to the O-terminated interface in our opinion (Fig. 3 in Ref. 56). W_{sep} of the $Ag/(Al_2O_3)_O$ interface is about 4–5 J/m^2. Even with some Ag atoms being left on the $(Al_2O_3)_O$ surface to saturate the surface oxygen dangling bonds and to neutralize the surface charge, W_{sep} is still about 2 J/m^2 [as indicated by $M/M(Al_2O_3)_O$ in Table III], higher than the W_{sep} of Ag bulk (about 1.5 J/m^2). Therefore, this interface is more likely to be broken in the silver bulk other than the real $Ag/(Al_2O_3)_O$ interface.

For the Au/Al_2O_3 interfaces, our calculations show that the Al-terminated interface is always the most stable one even after the P_{O_2} has been greater than 1 atmosphere [Fig. 6(b)] at 1400 K. By ignoring the area with $P_{O_2} > 1$ atmosphere, the Au/Al_2O_3 interface most likely has Al termination and shows no dependence of work of adhesion (or contact angle) on oxygen partial pressure. This is truly the experimental observation as reported by Chatain *et al.*[57]

2. Al_2-terminated interfaces

The results in Sec. IV B 1 showed that the Ag/Al_2O_3 interface may be Al or O terminated, and that the Au/Al_2O_3 interface is mostly Al terminated. The O termination is hardly observed for Au/Al_2O_3 interface. Although the interfacial energies of those interfaces depend on the interface type, i.e., the strain of the interfaces, as shown in Figs. 6(a) and 6(b), the general trend of the stability of the Al- and O-terminated $(Ag,Au)/Al_2O_3$ interfaces is unchanged. Such a trend is also in good agreement with experimental observation. Figures 6(a) and 6(b) also show that the Al_2-terminated interfaces may exist at low oxygen partial pressure for both the Ag/Al_2O_3 and Au/Al_2O_3 systems. To our knowledge, there is no reported experiment on the Al-rich interfaces for these systems. Our earlier calculations for Ag/Al_2O_3 interface using WIEN2K showed that the Al-rich interface had a bit higher interfacial energy than the Al-terminated one.[15] But careful inspection later showed that the configuration fell into a subtle local metastable state due to the complex interfacial structure. Further relaxation also reduced the interfacial energy to be lower than that of the Al-terminated one, similar to what we obtained in Fig. 6(a).

Due to the ideally commensurate interface model used in our calculations, whether the Al-rich $(Ag,Au)/Al_2O_3$ interfaces could exist is still a problem. By looking at the difference of the interfacial energies between the type-I and type-II interfaces of Al_2 termination, we notice that there may be an uncertainty (of about 0.3–0.4 J/m^2) of the interfacial energy for the Al_2-terminated systems. By taking that uncertainty into account and adding the number onto the calculated interfacial energy, the $Au/(Al_2O_3)_{Al2}$ interface still has lower energy than the $Au/(Al_2O_3)_{Al}$ interface. Therefore, the Al-rich interface may still exist for the Au/Al_2O_3 system. But the interfacial energy of the $Ag/(Al_2O_3)_{Al2}$ interface is no longer lower than that of the $Ag/(Al_2O_3)_{Al}$ interface, indicating that the $Ag/(Al_2O_3)_{Al2}$ interface may not be a stable state in practice. This is hardly conclusive because the interfacial energies of the Al-terminated interfaces may also have a uncertainty due to the strain effect. A good way is to study a real interface with misfit dislocation in the future.

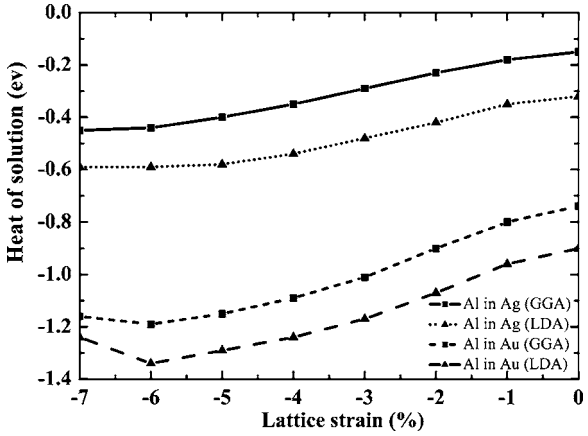

FIG. 8. Heats of solution for a substituional Al atom in the strained Ag and Au bulk.

We may also look at the problem from a different aspect. As discussed in Sec. III, the bonding at the Al_2-terminated interface is mainly determined by Ag-Al or Au-Al metallic interaction due to the extra Al layer at the interface than the Al-terminated interfaces. Therefore, change of the Al-Ag(Au) interaction with the strain of Ag(Au) may also provide hints on the extra uncertainty of the interfacial energy of such an Al-rich interface relative to the stoichiometric Al-terminated interfaces. To estimate the extra uncertainty, change of the heat of solution (HOS) for a substitutional Al atom in the strained Au or Ag bulk is calculated. The change of the HOS (per Al atom) is taken as a rough estimation of the extra uncertainty of the interfacial energy. Note that the Ag and Au lattices have the same strain (from −7% to 0) as the strain they have at the Al_2-terminated $(Ag,Au)/(Al_2O_3)_{Al2}$ interfaces. The aluminum heat of solution is defined as

$$\Delta H_{\text{solution}} = E_{\text{total}} - N_{\text{Ag}}\mu_{\text{Ag}}(\text{fcc}) - \mu_{\text{Al}}(\text{fcc}). \qquad (7)$$

E_{total} is the total energy of a supercell ($3\times3\times3$ of the primary unit cell of fcc metal) of silver bulk with an aluminum atom at a substitutional site. N_{Ag} is the number of silver atoms in the supercell, μ_{Ag} is the total energy (per atom) of pure silver at the strained state, and μ_{Al} is the total energy (per atom) of pure aluminum without strain. The $\Delta H_{\text{solution}}$ for Al in the strained Au is obtained by following the same procedure. Figure 8 shows the calculated HOS in both LDA and GGA. Note that the change of HOS with strain is not sensitive to LDA or GGA approach. For silver case, when Ag is compressed from 0 to −7%, the Al HOS goes deep and its change is 0.3 eV in either GGA or LDA. We may understand that a strained Ag slab or Au slab possibly enhances interfacial interaction and decreases interfacial energy. On the other hand, by mapping the change of HOS per Al onto the inter-

facial energy, we may get a rough estimation of uprising of the real interfacial energy. This is simple and by no means accurate. For the Al_2-terminated Ag/Al_2O_3 interface, the change of the interfacial energy is estimated to be 0.24 J/m^2. Such a change makes the interfacial energy of the Al_2-terminated Ag/Al_2O_3 interface be higher than that of the Al-terminated one, indicating that the Al_2-terminated interface is unlikely more stable than the Al-terminated one in practice. For gold case, the HOS change is about 0.4 eV with strain from 0 to −7% and the uprising of the interfacial energy is 0.33 J/m^2. It only changes a little the partial pressure for the Al_2-terminated interface to become stable. We believe that the Al_2-terminated Au/Al_2O_3 interface should be observable experimentally. The heat of solution for Al in Au is higher than that for Al in Ag, consistent with the above conclusion that the Al-rich interface may exist for the Au/Al_2O_3 interface but may not exist for the Ag/Al_2O_3 interface.

V. SUMMARY AND CONCLUSIONS

The structural stability and adhesion of the Ag/Al_2O_3 and Au/Al_2O_3 interfaces are studied by an *ab inito* method. Because of the lattice mismatch between metal Ag(Au) and alumina, two types of commensurate interfaces at different strained states, type I and type II, are studied parallelly. We trust only those results that are not sensitive to the interfacial strain. From the calculated interfacial energies, we conclude that the Al_2-terminated, O-terminated, and Al-terminated interfaces could exist depending on the environmental oxygen partial pressure. For Au/Al_2O_3, it is more likely that only the Al-terminated and Al_2-terminated interfaces could be observed. For conditions applicable to sessile drop experiments, the O-terminated interface could exist for the Ag/Al_2O_3 system but be hard to be observed for the Au/Al_2O_3 interfaces, consistent with the known experiments. The Al_2-terminated interface may exist for the Au/Al_2O_3 interfaces under relatively low O_2 pressure or high Al activity but may not exist for the Ag/Al_2O_3 interface. The chemical bonding of the O-terminated interfaces is more determined by the ionic interaction between metal and oxygen atoms, which leads to a strong adhesion of the interface. The bonding of Al-terminated interfacial is mainly determined by some metallic interaction mixing with electron polarization effect, leading to a relatively weak adhesion. The chemical bonding at the Al_2-terminated interface is metallic. Our calculated works of adhesion W_{ad} and works of separation W_{sep} show reasonable consistency with measured values.

ACKNOWLEDGMENTS

This work is supported by the National Natural Science Foundation of China under Grant No. 10474106 and the Information Construction of Knowledge Innovation Projects of Chinese Academy of Sciences "Supercomputing Environment Construction and Application" (Grant No. INF105-SCE).

[1] A. G. Evans D. R. Mumm, J. W. Hutchinson, G. H. Meier, and F. S. Pettit, Prog. Mater. Sci. **46**, 505 (2001).
[2] D. W. Goodman, Chem. Rev. (Washington, D.C.) **95**, 523 (1995).
[3] B. C. Gates, Chem. Rev. (Washington, D.C.) **95**, 511 (1995).
[4] C. C. Young, J. G. Duh, and C. S. Huang, Surf. Coat. Technol. **145**, 215 (2001).
[5] J. G. Li, Compos. Interfaces **1**, 37 (1993).
[6] C. Noguera, *Physics and Chemistry at Oxide Surfaces* (Cambridge University Press, Cambridge, 1996).
[7] C. T. Campbell, Surf. Sci. Rep. **27**, 3 (1997).
[8] G. Dehm, M. Rühle, G. Ding, and R. Raj, Philos. Mag. B **71**, 1111 (1997).
[9] G. Gutekunst, J. Mayer, and M. Rühle, Philos. Mag. A **75**, 1329 (1997).
[10] W. H. Gitzen, *Alumina as a Ceramic Material* (American Ceramic Society, Columbus, 1970).
[11] J. A. Kelber, C. Niu, K. Shepherd, D. R. Jennison, and A. Bogicevic, Surf. Sci. **446**, 76 (2000).
[12] J. Biener, M. Bäumer, R. J. Madix, P. Liu, E. Nelson, T. Kendelewicz, and G. E. Brown, Surf. Sci. **449**, 50 (2000).
[13] M. W. Finnis, J. Phys.: Condens. Matter **8**, 5811 (1996), and references cited therein.
[14] K. Reuter and M. Scheffler, Phys. Rev. B **65**, 035406 (2001).
[15] W. Zhang and J. R. Smith, Phys. Rev. Lett. **85**, 3225 (2000).
[16] W. Zhang, J. R. Smith, and A. G. Evans, Acta Mater. **50**, 3803 (2002).
[17] W. Zhang, J. R. Smith, and X.-G. Wang, Phys. Rev. B **70**, 024103 (2004).
[18] G. X. Qian, R. M. Martin, and D. J. Chadi, Phys. Rev. B **38**, 7649 (1988).
[19] I. N. Remediakis, E. Kaxiras, and P. C. Kelires, Phys. Rev. Lett. **86**, 4556 (2001).
[20] S. B. Zhang and J. E. Northrup, Phys. Rev. Lett. **67**, 2339 (1991).
[21] Y. Yan, S. B. Zhang, and S. T. Pantelides, Phys. Rev. Lett. **86**, 5723 (2001).
[22] J. Padilla and D. Vanderbilt, Phys. Rev. B **56**, 1625 (1997).
[23] X.-G. Wang, W. Weiss, Sh. K. Shaikhutdinov, M. Ritter, M. Petersen, F. Wagner, R. Schlogl, and M. Scheffler, Phys. Rev. Lett. **81**, 1038 (1998).
[24] X.-G. Wang, A. Chaka, and M. Scheffler, Phys. Rev. Lett. **84**, 3650 (2000).
[25] W. Zhang and J. R. Smith, Phys. Rev. B **61**, 16 883 (2000).
[26] I. G. Batyrev, A. Alavi, and M. W. Finnis, Phys. Rev. B **62**, 4698 (2000).
[27] I. G. Batyrev, A. Alavi, M. W. Finnis, and T. Deutsch, Phys. Rev. Lett. **82**, 1510 (1999).
[28] E. Saiz, R. M. Cannon, and A. P. Tomsia, Acta Mater. **47**, 4209 (1999).
[29] D. Chatain, L. Coudurier, and N. Eustathopoulos, Rev. Phys. Appl. **23**, 1055 (1988).
[30] J. E. McDonald and J. G. Eberhart, Trans. Metall. Soc. AIME, **233**, 512 (1965).

[31] *CRC Handbook of Chemistry and Physics*, 78th ed., edited by D. R. Lide (CRC Press, Boca Raton, FL, 1997).
[32] Yu. F. Zhukovskii, M. Alfredsson, K. Hermansson, E. Heifets, and E. A. Kotomin, Nucl. Instrum. Methods Phys. Res. B **141**, 73 (1998).
[33] Yu. F. Zhukovskii, E. A. Kotomin, B. Herschend, K. Hermansson, and P. W. M. Jacobs, Int. J. Mol. Sci. **2**, 271 (2001).
[34] Yu. F. Zhukovskii, E. A. Kotomin, B. Herschend, K. Hermansson, and P. W. M. Jacobs, Surf. Sci. **513**, 343 (2002).
[35] N. C. Hernández and J. F. Sanz, Appl. Surf. Sci. **238**, 228 (2004).
[36] G. Kresse and J. Furthmüller, Phys. Rev. B **54**, 11 169 (1996).
[37] G. Kresse and J. Hafner, Phys. Rev. B **47**, R558 (1993).
[38] G. Kresse and J. Hafner, J. Phys.: Condens. Matter **6**, 8245 (1994)
[39] D. Vanderbilt, Phys. Rev. B **41**, R7892 (1990).
[40] J. P. Perdew, in *Electronic Structure of Solids '91*, edited by P. Ziesche and H. Eschrig (Akademie Verlag, Berlin, 1991).
[41] J. P. Perdew and A. Zunger, Phys. Rev. B **23**, 5048 (1981).
[42] D. M. Ceperley and B. J. Alder, Phys. Rev. Lett. **45**, 566 (1980).
[43] D. J. Siegel, L. G. Hector, and J. B. Adams, Phys. Rev. B **65**, 085415 (2002).
[44] Ž. Crljen, P. Lazić, D. Šokčević, and R. Brako, Phys. Rev. B **68**, 195411 (2003).
[45] L. L Wang and H. P. Cheng, Phys. Rev. B **69**, 165417 (2004).
[46] A. Michaelides, M.-L. Bocquet, P. Sautet, A. Alaviand, and D. A. King, Chem. Phys. Lett. **367** 344-350 (2003).
[47] C. Kittel, *Introduction to Solid State Physics*, 4th ed. (Wiley, New York, 1971).
[48] J. R. Smith and W. Zhang. Acta Mater. **48**, 4395 (2000).
[49] W. Kohn and A. E. Mattsson, Phys. Rev. Lett. **81**, 3487 (1998).
[50] D. L. Medlin, K. F. McCarty, R. Q. Hwang, S. E. Guthrie, and M. I. Baskes, Thin Solid Films **299**, 110 (1997).
[51] G. Dehm, M. Ruhle, D. Ding, and R. Raj, Philos. Mag. B **71**, 1111 (1995).
[52] R. Benedek, A. Alavi, D. N. Seidman, L. H. Yang, D. A. Muller, and C. Woodward, Phys. Rev. Lett. **84**, 3362 (2000); J. Schnitker and D. J. Srolovitz, Modell. Simul. Mater. Sci. Eng. **6**, 153 (1998).
[53] Ralph W. G. Wyckoff, *Crystal Structure*, 2nd ed (Interscience, New York, 1964), Vol. 2.
[54] M. W. Chase, C. A. Davies, J. R. Downey, D. J. Frurip, R. A. McDonald, and A. N. Syverud, *JANAF Thermochemical Tables*, 3rd ed. [J. Phys.Chem. Ref. Data 14, 61 (1985)].
[55] O. Kubaschewski, C. B. Alcock, and P. J. Spencer, *Materials Thermochemistry*, 6th ed. (Pergamon, Oxford, 1993).
[56] D. Chatain, F. Chabert, V. Ghetta, and J. Fouletier, J. Am. Ceram. Soc. **77**, 197 (1994), and references cited therein.
[57] D. Chatain, F. Chabert, V. Ghetta, and J. Fouletier, J. Am. Ceram. Soc. **76**, 1568 (1993), and references cited therein.
[58] D. M. Lipkin, D. R. Clarke, and A. G. Evans, Acta Mater. **46**, 4835 (1998), and references cited therein.